Limiting Regimes of a Three-Dimensional Buoyant Hydraulic Fracture Emerging from a Point Source

Andreas Möri[1] and Brice Lecampion[1]

[1]Swiss Federal Institute of Technology Lausanne

November 23, 2022

Abstract

Buoyant hydraulic fractures occur in nature as magmatic dikes and sills. In industrial applications like well stimulation, the emergence of buoyant fractures is undesirable and often limited by the injected volume and/or variation of in-situ stress. This class of tensile fractures is governed by a buoyancy force resulting from the density contrast between the surrounding solid and the fracturing fluid. We focus here on fluid releases from a point source in an impermeable elastic media with homogeneous rock and fluid properties. The resulting buoyant force is thus constant. We combine scaling arguments and planar 3D hydraulic fracture growth simulations [1] to fully understand the emergence as well as the different propagation regimes of buoyant fractures. For a continuous release, a family of solutions dependent on a dimensionless-viscosity Mk$^{exists. In the limit of large toughness (Mk^{[?]}1), we retrieve a finger-like shape [2]. The stable breadth of the tail is generally akin to the PKN approximation presented in}$

Limiting Regimes of a 3D Buoyant Hydraulic Fracture Emerging from a Point Source

Andreas Möri, and Brice Lecampion

Geo-Energy Lab - Gaznat chair on Geo-energy, EPFL, Lausanne, Switzerland

Contacts: andreas.mori@epfl.ch, brice.lecampion@epfl.ch

GeoEnergyLab

Swiss National Science Foundation

1. Problem formulation

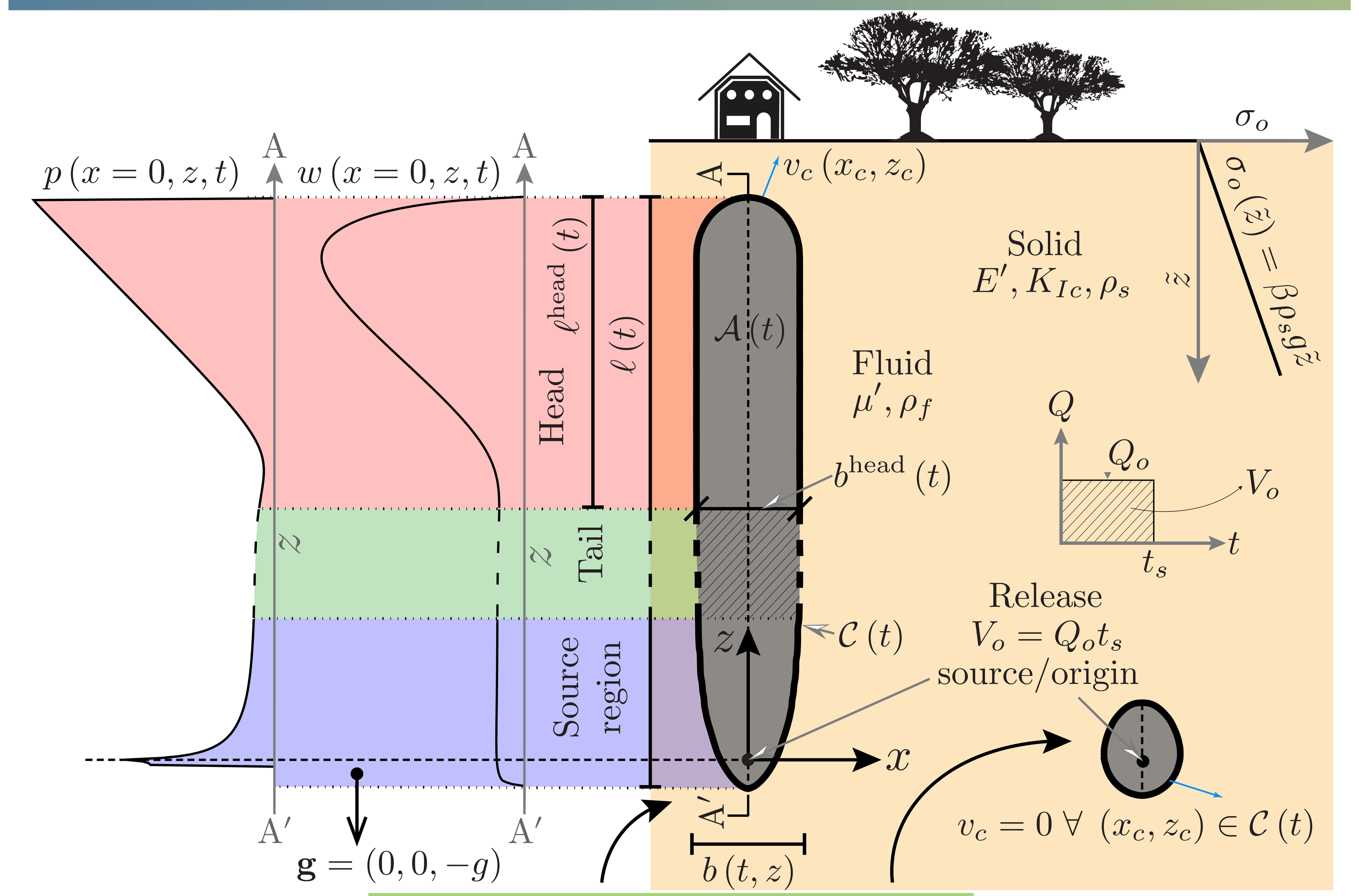

Does a self-sustained buoyancy-driven fracture emerge, or will the fracture arrest and remain at depth?

The problem of a planar mode I fracture assuming LEFM, no leak-off, and zero fluid-lag, is solved using PyFrac (Zia and Lecampion, 2020), an ILSA-based open-source solver. A scaling analysis reveals three main dimensionless coefficients

$$\mathcal{M}_{\hat{k}} = \mu' \frac{Q_o E'^3 \Delta\gamma^{2/3}}{K_{Ic}^{14/3}}, \quad \mathcal{B}_{\bar{k}} = \frac{\Delta\gamma E'^{3/5} V_o^{3/5}}{K_{Ic}^{8/5}}, \quad \mathcal{B}_{\bar{m}} = \frac{\Delta\gamma V_o^{1/3} t^{4/9}}{E'^{5/9} \mu'^{4/9}}$$

with $\Delta\gamma = (\beta\rho_s - \rho_f)\, g$. $\mathcal{M}_{\hat{k}}$ is a dimensionless viscosity parametrizing the continuous release and $\mathcal{B}_{\bar{k}}$ and $\mathcal{B}_{\bar{m}}$ dimensionless buoyancies parametrizing the finite volume release.

2. Continuous release, negligible toughness

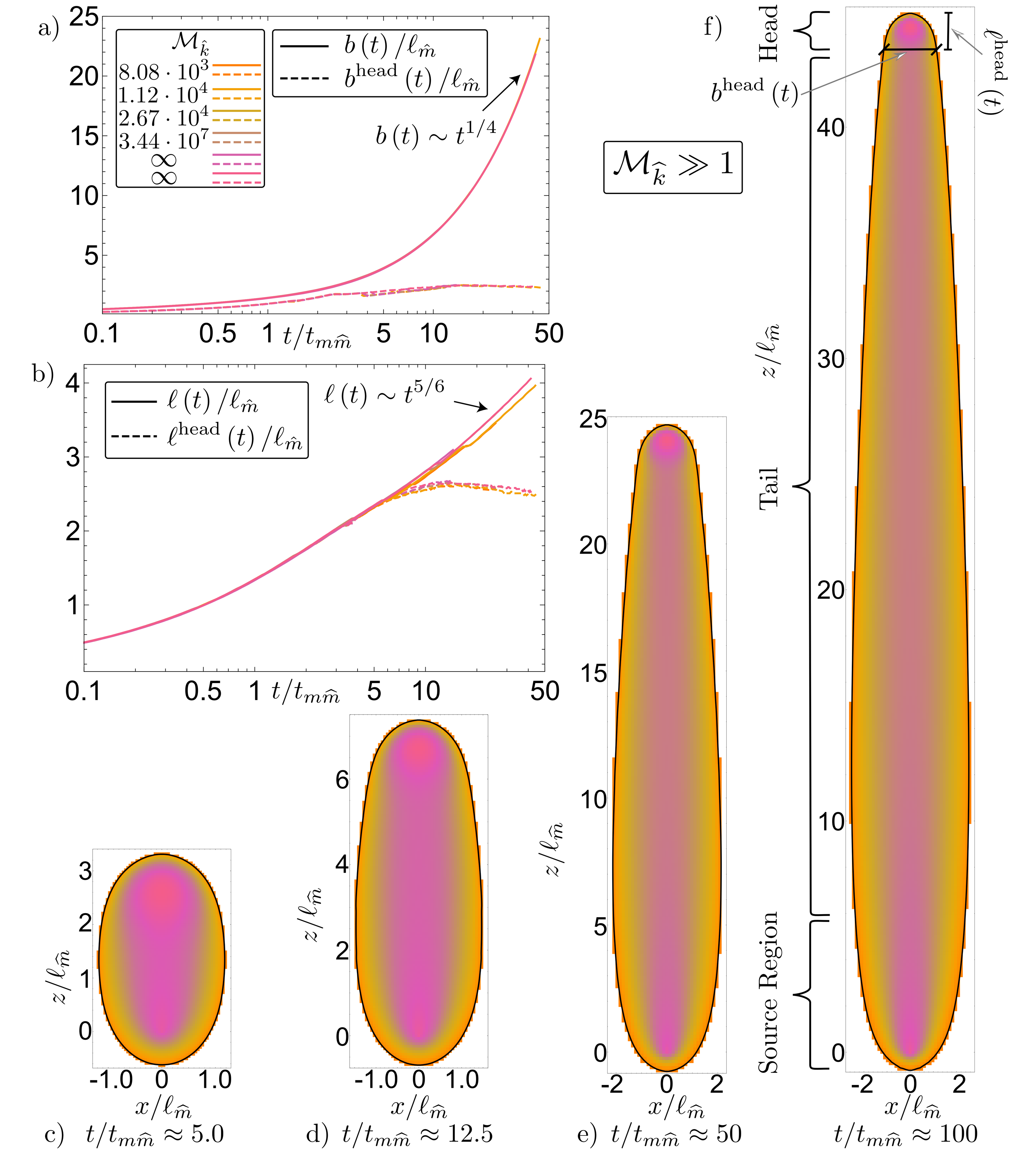

Evolution of a hydraulic fracture with a viscosity-dominated buoyant stage. A teardrop-shape with a increasing maximum breadth according to the pseudo-3D, zero-toughness prediction of Lister (1990) emerges. We indicate the corresponding power laws in time for the maximum breadth b and the fracture height ℓ in Figs. a) and b). A distinction in head ($\sim$ cst.), tail, and source region is possible. a) Maximum and head breadth. b) Head and total length. c-f) Footprints with opening distribution at different times. $t_{m\hat{m}}$ is the transition time from radial to buoyant, $\ell_{\hat{m}}$ the viscous buoyancy length-scale.

3. Continuous release, large toughness

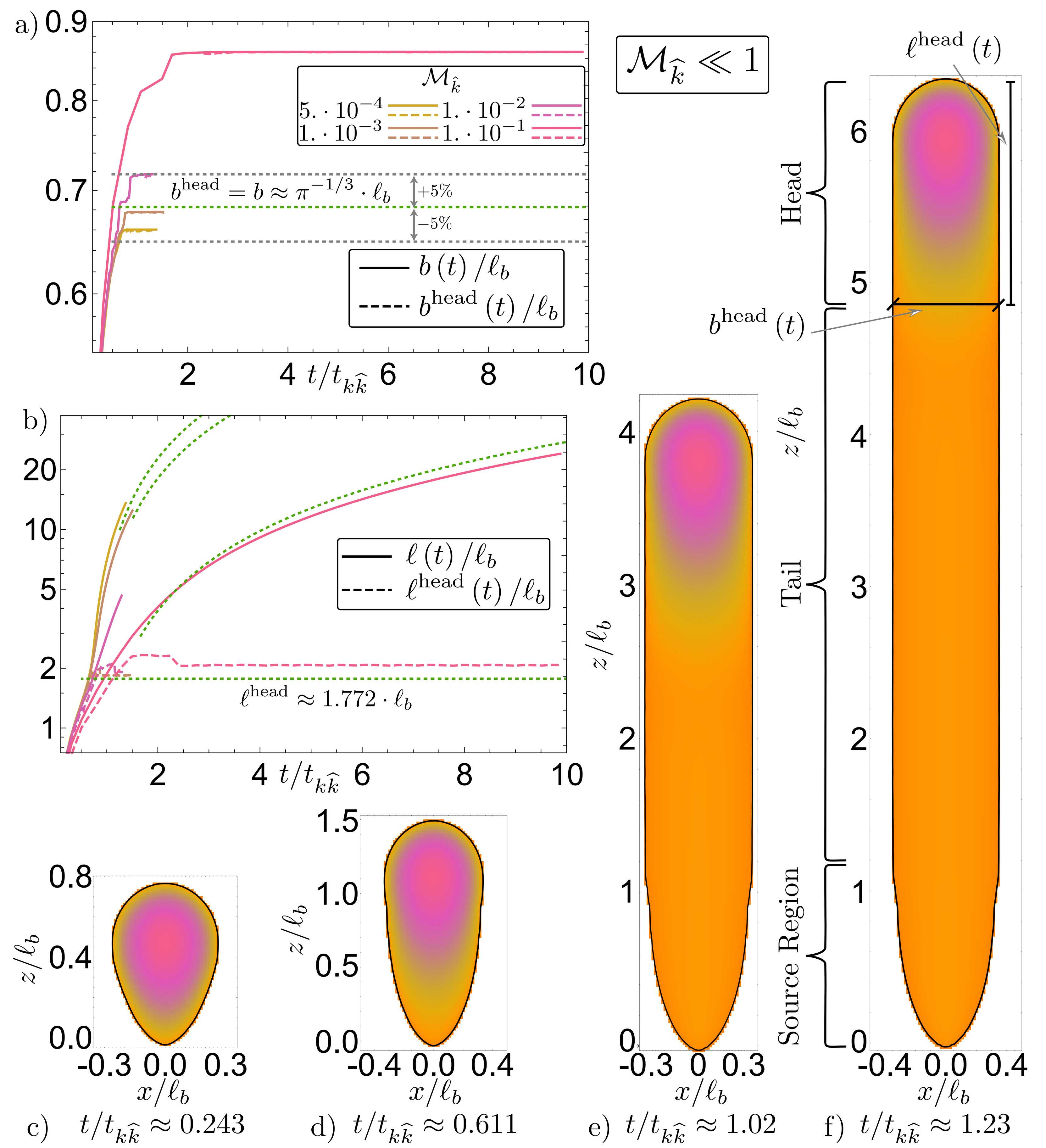

Evolution of a hydraulic fracture with a toughness-dominated buoyant stage. We validate the linear net pressure in the head, leading to a constant breadth of the fracture. Germanovich et al. (2014) derived a semi-analytical solution for this configuration, which we validate within numerical precision (green dotted lines). Their unique pre-factor on the stable breadth represents a zero-viscosity limit. Solutions with a larger stable breadth exist. The fracture form features a cst. head, an elongating tail, and a source region. a) Maximum and head breadth. b) Head and total length. c-f) Footprints with opening distribution at different times. $t_{k\hat{k}}$ is the transition time from radial to buoyant, ℓ_b the buoyancy length-scale (Lister and Kerr, 1991).

4. Pulse release, arbitrary toughness

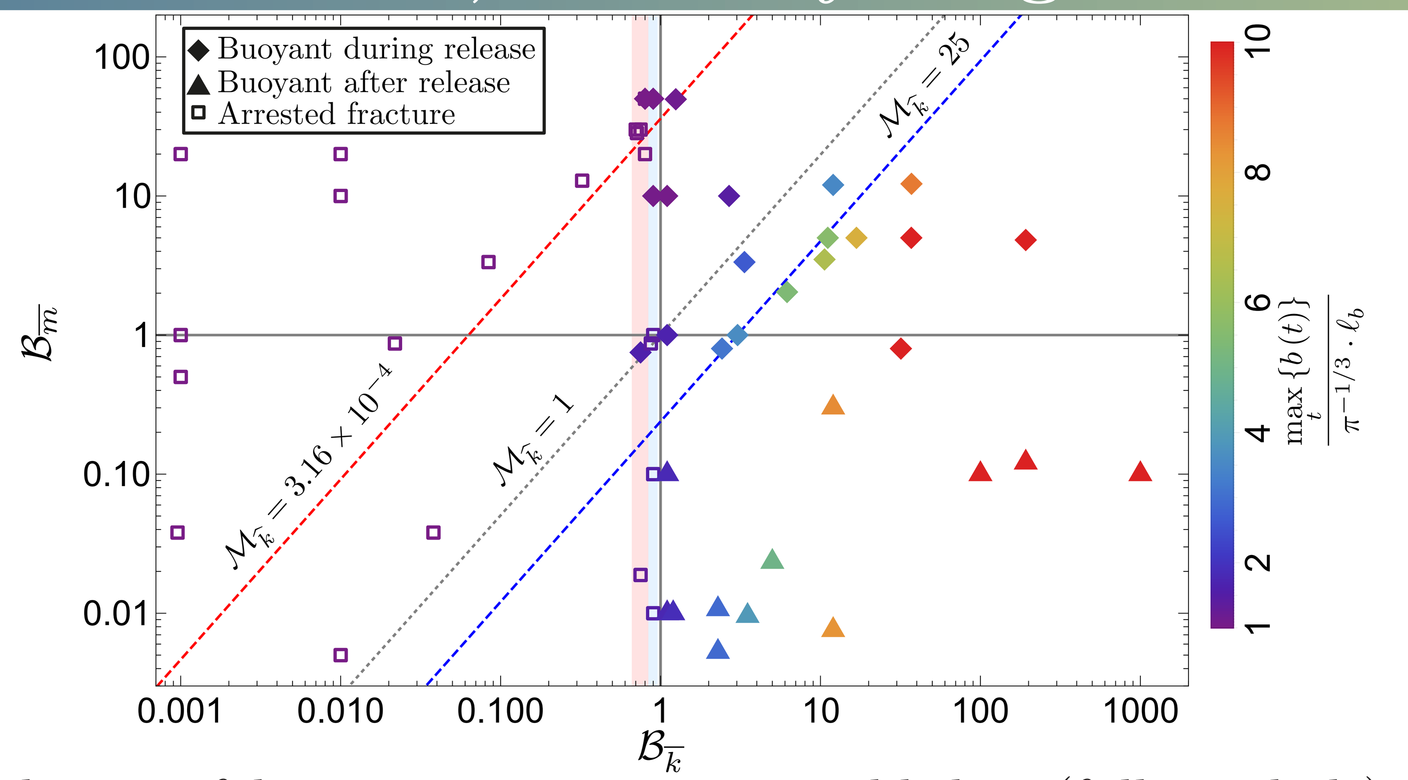

$\mathcal{B}_{\bar{k}}$ indicates if buoyant propagation establishes (full symbols). At late time, the head breadth approaches the zero-viscosity limit. The color code shows the fraction between maximum and limiting breadth. Various general shapes for the final buoyant crack exist, the shape is largely dominated by a combination of $\mathcal{B}_{\bar{k}}$ (x-axis) and $\mathcal{B}_{\bar{m}}$ (y-axis).

5. Conclusions

- During the release, a family of solutions in function of $\mathcal{M}_{\hat{k}}$ with two limiting regimes emerges. The toughness limit is akin to a finger-like / blade-shaped fracture || the viscous limit has a teardrop shape with an increasing maximum breadth.
- For a finite volume release, a self-sustained, buoyancy-driven crack emerges if $\mathcal{B}_{\bar{k}} \geq 1$. Its shape additionally depends on $\mathcal{B}_{\bar{m}}$.
- Most geotechnical and natural applications have negligible toughness or are in between the limits and have $\mathcal{B}_{\bar{k}} > 1$.

For more information and references, see the online version of the poster or check our labs' webpage for publications (see QR-codes).

Take home message

Calculating a **single coefficient** $\mathcal{B}_{\bar{k}}$ from solid, fluid, and release properties is sufficient to know if a **buoyancy-driven, self-sustained** fracture emerges.